Pergamon

Geochimica et Cosmochimica Acta, Vol. 68, No. 11, pp. 2437–2448, 2004

0016-7037/04 $30.00 + .00

doi:10.1016/j.gca.2003.09.023

Spectroscopic investigation of U(VI) sorption at the calcite-water interface

EVERT J. ELZINGA,[1,*] C. DREW TAIT,[2] RICHARD J. REEDER,[1] KIRK D. RECTOR,[3] ROBERT J. DONOHOE,[3] and DAVID E. MORRIS[2]

[1]Department of Geosciences and Center for Environmental Molecular Science, State University of New York at Stony Brook, Stony Brook, New York 11794-2100 USA

[2]Chemistry Division, G. T. Seaborg Institute for Transactinium Science, Los Alamos National Laboratory, Los Alamos, New Mexico 87545 USA

[3]Biosciences Division, G. T. Seaborg Institute for Transactinium Science, Los Alamos National Laboratory, Los Alamos, New Mexico 87545 USA

(*Received June* 3, 2003; *accepted in revised form September* 16, 2003)

Abstract—The interaction of U(VI) species with the calcite surface in pre-equilibrated calcite suspensions at pH 7.4 and 8.3 and $P(CO_2) = 10^{-3.5}$ bar was characterized in situ using extended X-ray absorption spectroscopy (EXAFS) and luminescence spectroscopies. Results indicate that uranyl triscarbonate-like adsorption complexes dominate at U(VI) solution concentrations <500 μM, whereas the formation of U(VI) hydroxide and carbonato precipitates is observed at higher concentrations, consistent with isotherm data and aqueous speciation calculations. The EXAFS data indicate weak splitting in the equatorial O shell of the U(VI) adsorption complexes, which may indicate that the adsorption complexes are bound in an inner-sphere fashion at the calcite surface, although no Ca backscattering could be positively identified. The luminescence data indicate the presence of at least two adsorption complexes that change proportion with U(VI) loading. One species, dominating at low-surface coverage, is the uranyl triscarbonate complex. A second species is observed at higher surface loadings with a luminescence spectrum that is intermediate between the triscarbonate species found at the lowest loadings and uranyl incorporated into bulk polycrystalline calcite. The combined EXAFS and luminescence data indicate that the U(VI) adsorption complexes forming at the calcite surface are triscarbonate-like complexes, with a change in interaction with calcite surface sites as the surface loading increases, and the formation of U(VI) hydroxide/carbonato precipitates at high concentrations. Consequently, multiple uranyl species are likely to exist at the calcite surface during interaction of U(VI)-containing waters in the near-surface environment. Furthermore, complex sorption/desorption behavior and kinetics may be associated with differing stabilities of sorbed U(VI) species in calcite-containing materials. *Copyright © 2004 Elsevier Ltd*

1. INTRODUCTION

Sorption of U(VI) by minerals and organic matter may be one of the dominant mechanisms that limits the mobility of this radionuclide in soil- and sediment-water systems. The effectiveness and mechanism of sorption and the stability of the sorbed species determine the retention of the contaminant and are therefore critical for predicting the long-term fate of this radionuclide. U(VI), the stable oxidation state in oxidized surface environments, exists almost exclusively as the uranyl species (UO_2^{2+}) at surface conditions and generally exhibits solubility and mobility far exceeding that of U(IV), the other common oxidation state (Langmuir, 1997). Sorption of uranyl by minerals depends on numerous factors, including the nature and availability of surface binding sites, solution composition and pH, and aqueous complexation. The presence of dissolved ligands may strongly influence uranyl speciation, thereby either increasing or decreasing uptake behavior. Carbonate is widely regarded as an important ligand owing to its near ubiquitous presence in surface waters as well as to the stability of uranyl carbonate complexes. In carbonate-containing waters above pH 6, carbonate complexes typically dominate the aqueous speciation of U(VI) and may significantly enhance U(VI) solubility. Precipitation of U(VI)-containing phases can provide limits for U(VI) solubility, but phases likely to form in carbonate-containing systems [e.g., rutherfordine (UO_2CO_3), liebigite ($Ca_2(UO_2)(CO_3)_3 \cdot 11H_2O$), schoepite ($UO_3 \cdot 2H_2O$), and β-$UO_2(OH)_2$] exhibit moderate solubilities under a range of conditions typical for soil and sediment systems, thereby providing only modest constraints to total dissolved U(VI) concentrations.

Uranyl has been shown to interact strongly with several important mineral components of soils and sediments, including iron and manganese oxides and hydroxides, clays, and other silicates (e.g., Hsi and Langmuir, 1985; Morris et al., 1994; McKinley et al., 1995; Payne et al., 1998). Relatively few studies have addressed uranyl interaction with calcium carbonate phases. The most abundant calcium carbonate phase, calcite ($CaCO_3$), is particularly widespread in occurrence and is known to be highly effective as a sorbent for a variety of dissolved metal species. Calcite-saturated waters in the pH range 7 to 8.5 typically have total dissolved carbonate/bicarbonate concentrations in the range 10^{-4}–10^{-3} M, ensuring that uranyl carbonate complexes are dominant in such solutions. Studies of uranyl sorption on goethite, ferrihydrite, hematite, kaolinite, and clinoptilolite (Waite et al., 1994; Pabalan et al., 1998; Lenhart and Honeyman, 1999) have demonstrated that a broad uptake maximum typically occurs over the near-neutral pH range (for systems in contact with air). At higher pH values, decreased sorption is associated with increasing dominance of uranyl carbonate complexes in solution, suggesting that these complexes show a relatively low affinity for binding at oxide,

* Author to whom correspondence should be addressed (eelzinga@notes.cc.sunysb.edu).

hydroxide and aluminosilicate surface sites. However, the studies of Bargar et al. (1999, 2000) provide evidence that carbonate ligands play a role in uranyl sorption at the hematite-water interface. Using extended X-ray absorption fine-structure (EXAFS) spectroscopy, their results indicate that uranyl forms ternary Fe-oxide–UO_2^{2+}–CO_3^{2-} surface complexes over a wide range of pH conditions.

Variably-protonated carbonate units are expected to be among the functional groups at the calcite surface in solution (cf., Fenter et al., 2000). Questions that immediately arise are whether and how such surface groups might provide favorable coordinative sites for binding of uranyl at the calcite-water interface. Such surface sites can be viewed as competing with dissolved carbonate to stabilize the uranyl species. The presence of significant amounts of dissolved Ca^{2+} in calcite-saturated solutions may also influence uranyl sorption behavior by calcite. Bernhard et al. (1996, 2001) and Kalmykov and Choppin (2000) showed that the neutral $Ca_2UO_2(CO_3)_3$ aqueous species may be important in calcium- and carbonate-rich waters. Speciation simulations using reported stability constants show that this complex is stable over a broad range of U(VI), Ca, and carbonate concentrations, indicating that uranyl carbonate complexes have a high affinity for binding with Ca^{2+} (and presumably other divalent metals). Because both filled and unfilled Ca sites are exposed at the calcite-water interface, uranyl sorption can also be viewed as the affinity of uranyl carbonate complexes for coordinating with surface-bound Ca atoms.

Insight to the sorption mechanisms of uranyl species is also important for understanding surface controls on U(VI) coprecipitation with calcite and aragonite. Recent studies (Reeder et al., 2000, 2001) have demonstrated that significant amounts of uranyl can be incorporated into calcite and aragonite during laboratory coprecipitation experiments. An important observation is that uranyl is incorporated differentially between nonequivalent growth steps on the common $(10\bar{1}4)$ face of calcite (Reeder et al., 2001). Several studies have demonstrated that multiple sites exist on this surface and are segregated between two pairs of nonequivalent vicinal faces during spiral growth (Paquette and Reeder, 1995; Reeder, 1996). In uranyl coprecipitation experiments with calcite single crystals, uranyl is found to be preferentially taken up at the steps in the "-" vicinal faces (Reeder et al., 2001). The significance of this observation is that incorporation is strongly influenced by detailed characteristics of surface sites in steps; this suggests that the discrimination is associated with the coordinative aspects of the adsorbed uranyl species. Potential binding sites also exist on $(10\bar{1}4)$ terraces, so that multiple types of surface sites are available for adsorption on calcite.

In the present study we investigate the interaction of U(VI) species at the calcite-water interface in an effort to determine the identity and coordination of sorbed uranyl species. Samples prepared in batch uptake experiments at pH 7.4 and 8.3 are examined in situ using EXAFS and luminescence spectroscopies, which allow us to characterize the local coordination of sorbed species and deduce mechanisms of uptake. Careful attention is given to maintaining equilibrium and constant pH in the calcite-water suspensions to avoid or minimize the potential for dissolution/precipitation and coprecipitation. Our findings reveal complex sorption processes at the calcite-water interface, with at least two uranyl species being important.

2. PRIOR STUDIES OF U(VI) INTERACTION WITH CALCITE

Most of the previous work on uranyl interaction with calcite has characterized the uptake behavior in batch studies. Morse et al. (1984) observed an unusual sorption/desorption behavior in batch experiments of uranyl uptake by calcite from solutions preequilibrated with calcite at atmospheric $P(CO_2)$, and then spiked with uranyl concentrations ranging between 24 μM and 3.2 mM. Rapid initial uptake over periods up to 30 min was followed by complete or extensive desorption over a longer time scale (up to 165 h). In their experiments, the sorption became most significant when UO_2^{2+} concentrations were comparable in magnitude to the carbonate alkalinity, suggesting that formation of uranyl carbonate complexes played a role in the sorption/desorption sequence, for example, a change in aqueous uranyl speciation from hydroxy to carbonato complexes. An important implication of this study is that addition of UO_2^{2+} to a calcite-containing system may result in dissolution of calcite to supply carbonate ligands for uranyl complexation in solution.

Carroll and Bruno (1991) examined U(VI) interaction with the calcite surface in batch experiments using calcite-saturated solutions. Over the range of $P(CO_2)$ (0.001–0.9 bar), pH (5.4–7.5), and uranyl solution concentrations ($\sim 10^{-4}$–10^{-2} M) conditions studied, they found that uranyl exhibits limited adsorption at the calcite surface with approximately 90% of the sorbed uranyl readily desorbable. No evidence of coprecipitation was found over the range of U(VI) concentration studied. The adsorption of UO_2^{2+} was modeled as an exchange with surface Ca^{2+} and assumed formation of a $>UO_2CO_3$ surface species. Savenko (2001) also examined U(VI) sorption on calcite in batch experiments conducted at atmospheric $P(CO_2)$ and pH values of 7.45–7.8, and found the isotherm to be linear over the range 2–10 μM total U(VI). Uptake was also found to be linear with the solution UO_2^{2+}/Ca^{2+} ratio, and adsorption was modeled as an exchange with surface Ca^{2+}. At higher U(VI) concentrations, exceeding the solubility of rutherfordine (UO_2CO_3), Carroll et al. (1992) observed formation of U-containing and Ca-containing precipitates at the calcite-water interface in a calcite-saturated solution (pH 8.0) spiked with a uranyl concentration of 0.22 mM. Kaplan et al. (1998) conducted batch experiments to characterize U(VI) interaction with natural calcite-containing sediments, using uranyl concentrations between 3.3 and 100 μg L^{-1}, and a pH range of 8.3 to 12.0. Their results revealed limited U(VI) uptake below pH 10.3; above this pH they observed significantly increased uptake, which was attributed to precipitation or coprecipitation. Geipel et al. (1997) used X-ray photoelectron spectroscopy (XPS) and EXAFS to characterize the speciation of uranyl reacted with calcite in free-drift batch experiments conducted at atmospheric $P(CO_2)$ and at pH values in the range 8.2 to 8.9. Although spectroscopic measurements were made ex situ (after samples were rinsed and dried), they provide evidence suggesting that U(VI) occurred both as a uranyl hydroxide precipitate and as uranyl exchanged with Ca sites.

3. EXPERIMENTAL METHODS

3.1. Sorption Experiments

Experiments used a calcite sorbent with an average particle size of 1.8 μm and a N_2-BET surface area of $\sim$10 m^2 g^{-1}. The calcite was obtained from Spectrum Laboratory Chemicals, and suspensions were prepared as described below. In all experiments, calcite-saturated solutions were used to prevent calcite dissolution or precipitation during the sorption experiments. The majority of experiments were performed at pH 8.3. For these experiments, we used calcite-water suspensions of 0.5 or 1.0 g L^{-1} that had been equilibrated at atmospheric $P(CO_2)$ (i.e., saturated air was continuously bubbled through the suspension) for $\sim$3 weeks at room temperature, yielding an equilibrium pH of 8.3. Another set of experiments was done at pH 7.4. Solutions for these suspensions were prepared by air-equilibrating calcite in water containing a predetermined amount of HCl. The HCl concentrations needed to achieve pH 7.4 in the calcite-equilibrated solutions were calculated using PHREEQC (Parkhurst and Appelo, 1999). Following equilibration (4 weeks), the suspensions were filtered to collect the solutions. Fresh calcite was added to the solutions at a particle loading of 0.5 g L^{-1}, and the suspensions were equilibrated in air for another 3 weeks before reaction with uranium.

Uranium(VI) sorption experiments were performed at U solution concentrations ([U]) ranging from 5 μM to 5 mM. To prevent calcite dissolution upon the addition of U(VI) as a result of uranyl-carbonate complexation in solution (as observed by Morse et al., 1984), we used a stock solution consisting of 0.04 mol/L U(VI) and 0.1 mol/L Na_2CO_3, where U(VI) exists mainly (70%) as the triscarbonate complex, $UO_2(CO_3)_3^{4-}$.

An isotherm for U(VI) adsorption on calcite was measured to determine the overall U(VI) uptake by calcite as a function of [U]. Equilibrated calcite-water suspensions (pH 8.3) with a particle loading of 1.0 gL^{-1} were used for these experiments. Duplicate samples of 200 mL were spiked with [U] ranging from 10 μM to 3 mM by adding appropriate amounts of the 0.04 mol/L U(VI) stock solution. The pH increased upon the addition of U (especially at the higher concentrations) and was readjusted to the initial value using 0.1 mol/L HCl within 5 min following the U(VI) spike. The samples were equilibrated on a reciprocal shaker for 3 d. The final suspension pH values were measured, and the samples were vacuum filtered through 0.22 μm filter paper. A 5 mL volume of U-free calcite-saturated solution was filtered through the calcite 'cake' remaining on the filter to remove U(VI) present in entrained electrolyte solution; analyses of the U(VI) concentration of the rinsates indicated that this treatment removed entrained solution U(VI) and that no significant desorption occurred during this brief rinsing. The solids were then oven dried at 60°C, weighed, and dissolved in 5 mL volumes of concentrated HNO_3. The resulting solutes were analyzed for dissolved U using direct current plasma (DCP) spectrometry. Uranium(VI) uptake was calculated from the solute U concentration and the amount of solid dissolved. Final U(VI) solution concentrations in the sorption samples were calculated from the initial U concentration and the amount of U sorbed.

EXAFS and luminescence samples were prepared using calcite suspensions of 0.5 g L^{-1}. The samples were spiked with [U] ranging between 5 μM and 5 mM, with addition of 0.1 mol/L HCl to readjust pH as necessary. The samples were equilibrated on a reciprocal shaker for 3 d, measured for pH, and then filtered through 0.22 μm filter paper to a consistency of wet paste to preserve sorption complexes. For two samples, U was added from a stock containing only UO_2^{2+} and NO_3^- (and no Na_2CO_3), to evaluate the effect of carbonate co-addition at [U] = 50 and 500 μM, and pH 8.3.

3.2. EXAFS Spectroscopy

Wet pastes recovered from the sorption experiments were immediately mounted in lucite or Kel-F sample holders and sealed using a thin layer of Kapton or Kel-F to prevent drying of the sample. The final suspension pH values in the equilibrated samples were between 8.3 and 8.6, with the slightly higher pH values of 8.5 and 8.6 found for the highest U(VI) concentrations. Because uptake of uranyl by calcite is limited, we assessed the amount of residual uranium in the small amount of fluid remaining in the sample cells. In all cases, the amount of uranium in the entrained solution was estimated to contribute $<$5% to the total amount of U in the sample, as determined from mass balance calculations taking into account the amount of entrained electrolyte per mass of calcite powder, the U solution concentration, and the amount of sorbed U. The EXAFS data are therefore dominated by sorbed U and the contribution from U remaining in solution is negligible.

All EXAFS spectra were collected at ambient conditions at the bending-magnet beam line at sector 12 at the Advanced Photon Source, operated by BESSRC. The beam was used in a defocused mode to give a spot size on the sample of approximately 1 $\times$ 2 mm. A pair of Si(111) crystals was used in the monochromator, with the second crystal detuned typically by 15 to 20%. Sample cells were mounted at 45° to the incident beam, and spectra were measured in fluorescence mode using a Canberra 13-element solid-state Ge detector positioned at 90° to the beam. For samples with high sorbed U loadings, multiple layers of aluminum foil were placed in front of the detector window to reduce the fluorescence count rates. Multiple scans (between 5 and 20) were taken for each sample. Following data collection, sample cell windows were briefly opened in an appropriate lab to confirm that uranyl-sorbed calcite pastes retained their moisture. Cells were immediately resealed and saved for luminescence measurements. EXAFS spectra were also collected for the aqueous uranyl triscarbonate species in liquid cells. EXAFS spectra of U(VI) coprecipitated with calcite and aragonite were available from previous studies (Reeder et al., 2000, 2001).

Individual EXAFS scans were checked for energy calibration and for any indication that spectra changed over the duration of scanning, and then averaged. Background subtraction and normalization used a linear preedge function and a second-order postedge polynomial. E_0 was assigned the value 17171 eV. The χ function was extracted using a cubic spline with k^3 weighting. All fitting was done using the program WinXAS (Ressler, 1997) and theoretical phases and backscattering amplitudes calculated using FEFF7 (Ankudinov and Rehr, 1997).

Fitting was done in *R*-space on the Fourier transforms of the k^3-weighted χ spectra. The typical k and R ranges were 3 to 12.5 $Å^{-1}$ and 0.6 to 4.5 Å, respectively. Most samples had EXAFS data resembling that of the uranyl triscarbonate complex (as shown in the results) and were fit with 6 shells. To reduce the number of free parameters in the initial fitting procedure, we fixed the coordination number of each shell at the value consistent with the uranyl triscarbonate complex, having three bidentate CO_3 groups in the equatorial plane. The amplitude reduction factor, S_0^2, was set at 1, and a global threshold energy, E_0, was allowed to vary during fitting, along with the radial distances and Debye-Waller factors of each shell. One of the paths included in fitting was a multiple scattering (MS) contribution among the two axial O atoms of the uranyl moiety; the Debye-Waller factor for this MS shell was constrained to be twice that of the (floating) U-O_{axial} correlation. Errors for the fit parameters were estimated on the basis of comparisons of fit results for well-characterized model compounds with structure parameters determined from XRD analyses. Estimated errors for radial distance (R) are $\pm$0.01 Å for first and second shells, and $\pm$0.02–0.04 Å for more distant shells. Errors for the Debye-Waller factors are estimated at $\pm$0.001–0.002 $Å^2$.

3.3. Luminescence Spectroscopy

Time-resolved luminescence spectra of the uranyl-sorbed samples were collected using a SPEX Industries Fluorolog 2 system with a Model 1934D phosphorimeter attachment for the flashlamp excitation source (400–420 nm) as described elsewhere (Clark et al., 1999). The detection window was gated from 0.05 to 2.0 ms unless otherwise stated. The afterglow from the flashlamp extends to $\sim$0.05 ms precluding the collection of time-resolved data at times shorter than this. All samples were cooled to liquid nitrogen temperatures for luminescence work.

Spatially-resolved fluorescence spectra were also collected from a uranyl-doped single-crystal calcite sample prepared as described in the study by Reeder et al. (2001). The method used to collect this spectrum will be described in a subsequent paper. Briefly, single crystal images were acquired using a custom-built hyperspectral fluorescence/Raman microscope. The system cylindrically focuses $\sim$5 mW of a 458 nm excitation source into a Carl Zeiss Axiovert 135TV inverted microscope. The resulting fluorescence passes through a Kaiser Optical 458

supernotch filter to remove the excitation light and re-images the excitation profile onto the entrance slit of a Kaiser Holospec spectrometer. Resulting light is defracted onto a Roper Scientific CCD camera, where each frame captures one spatial and one spectral axis of the image. The resulting spatial axis is acquired by moving a Cell Robotics motorized microscope stage. The resulting hyperspectral image has spatial resolution of <1 μm and a spectral resolution of <1 nm.

3.4. UO_2^{2+} Speciation Calculations

Aqueous uranyl speciation was calculated for the initial conditions in the suspensions using the program PHREEQC (Parkhurst and Appelo, 1999) and the thermo.com.V8.R6.230 database prepared by Jim Johnson at Lawrence Livermore National Laboratory. The stability constants for U(VI) species are generally consistent with those in the Nuclear Energy Agency database (Grenthe et al., 1992). The neutral $Ca_2UO_2(CO_3)_3$ species reported by Bernhard et al. (1996, 2001) and Kalmykov and Choppin (2000) was also included (log K_0 = 30.55; Bernhard et al., 2001). Uranyl speciation was calculated as a function of the uranyl concentration (with co-added CO_3) in solutions in equilibrium with calcite at pH 8.3 and pH 7.4 at $P(CO_2) = 10^{-3.5}$ bar. This corresponds to the solution conditions for the majority of the sorption experiments. In another set of calculations, U was added (without co-addition of CO_3) to solutions of (fixed) pH 8.3 and with Ca and total carbonate concentrations fixed at the concentrations of those in calcite-saturated solutions of pH = 8.3 and $P(CO_2) = 10^{-3.5}$bar, to evaluate the effect of U-CO_3 solution complexation on calcite and U precipitate saturation states.

3.5. X-ray Powder Diffraction Measurements

X-ray diffraction (XRD) patterns were obtained for two sorption samples reacted with 2.5 mM U(VI): one in which carbonate was co-added with U(VI) and the other where U(VI) was added without CO_3. XRD data were obtained using a Scintag diffractometer (Cu $K\alpha$ radiation) with a Ge detector. Wet paste samples from adsorption experiments were allowed to air-dry completely, then powders were disaggregated and ground in acetone and thin films were allowed to dry on low-background quartz plates. Intensity data were collected over the range 5 to 50° or 10 to 60° (two theta) using a step interval of 0.02° and counting time of 6 s/step.

4. RESULTS

4.1. UO_2^{2+} Speciation in the Calcite Suspensions

The aqueous U speciation at pH 8.3 and pH 7.4 in calcite-saturated solutions is dominated by the neutral $Ca_2UO_2(CO_3)_3$ species over the [U] range used in this study, as shown in Figure 1. This species has a configuration essentially the same as the uranyl triscarbonate species [$UO_2(CO_3)_3^{4-}$] with two Ca atoms bridging equatorial oxygens of adjacent CO_3 groups, much as in the mineral liebigite (Bernhard et al., 2001). The neutral $Ca_2UO_2(CO_3)_3$ species remains most abundant over the entire [U] range, but the dimeric $(UO_2)_2CO_3(OH)_3^-$ species becomes increasingly important with increasing [U], accounting for as much as 40% of the uranyl at a total U(VI) concentration of 5 mM (Fig. 1a). At pH 7.4 the $Ca_2UO_2(CO_3)_3$ species accounts for $>95\%$ of total aqueous uranyl over the entire [U] range, due to the higher Ca concentration at this lower pH.

Calcite-saturated suspensions of pH 8.3 spiked with total U(VI) concentrations greater than approximately 500 μM were supersaturated with respect to β-$UO_2(OH)_2$ and schoepite (Fig. 2). Calculations on U(VI) added (without co-addition of CO_3) to solutions of fixed pH 8.3 and with Ca and total carbonate concentrations fixed at the concentrations of those in calcite-saturated solutions of pH = 8.3 and $P(CO_2) = 10^{-3.5}$ bar indicate that oversaturation with respect to β-$UO_2(OH)_2$ and schoepite is reached at significantly lower U concentrations than in the calcite-saturated solution of pH 8.3 (Fig. 2). The limited amount of carbonate in these systems prevents the formation of (relatively stable) triscarbonate U(VI) solution complexes at higher [U]. This indicates that U-CO_3 solution complexation stabilizes U(VI) against precipitation.

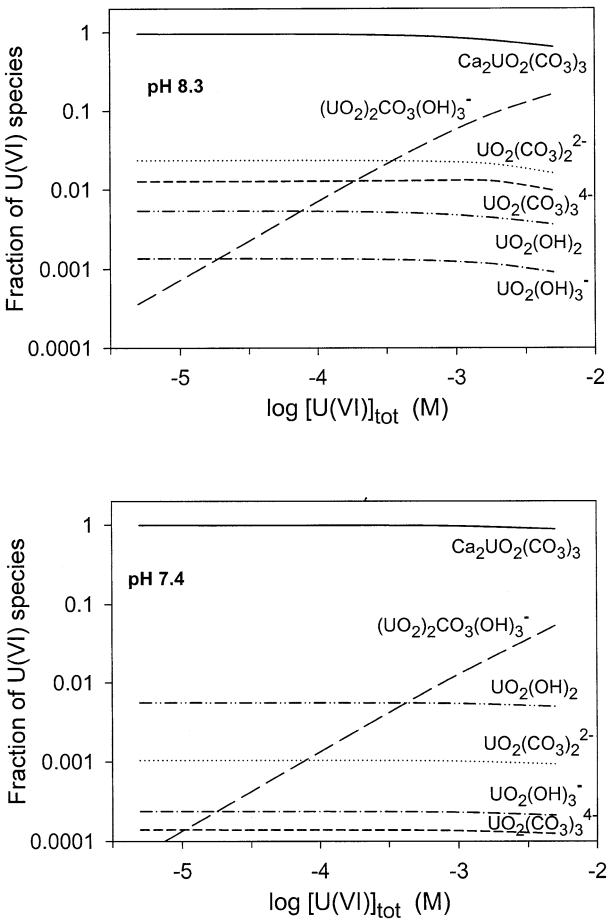

Fig. 1. Aqueous U(VI) speciation in calcite-saturated solutions of pH 8.3 and pH 7.4 at atmospheric $P(CO_2) = 10^{-3.5}$ bar as a function of U(VI) concentration.

4.2. Sorption Isotherm

The U(VI)-calcite sorption isotherm is shown in Figure 3. The suspension pH of the samples used in this experiment were in the range 8.3 to 8.6, and carbonate was co-added with U(VI) in all cases. Uranyl uptake increases with the U solution concentration and shows no evidence of reaching a Langmuir sorption plateau, although there is a decrease in fractional uptake with [U] at concentrations <500 μM. The sharp rise in U(VI) removal from solution at concentrations >500 μM suggests precipitation in the high [U] range, consistent with the speciation calculations presented above.

4.3. X-ray Powder Diffraction of Selected Sorption Samples

Figure 4 shows the XRD patterns of the calcite powders reacted with 2.5 mM U(VI) in the absence and presence of

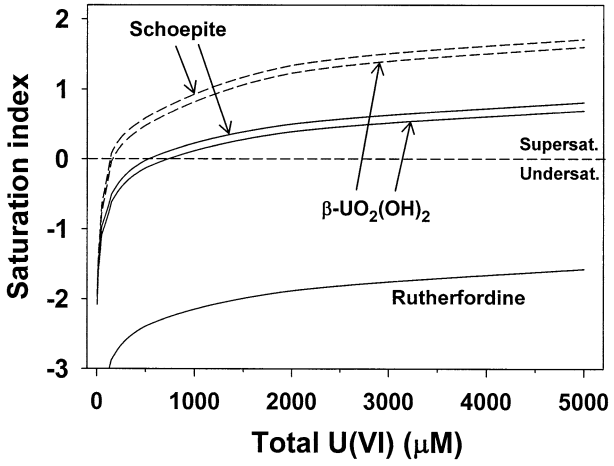

Fig. 2. Saturation index values of possible precipitate phases as a function of the U(VI) solution concentration. Calculations carried out for calcite-saturated solutions of pH 8.3 are presented by the solid curves. Dashed lines indicate calculations on U(VI) added as uranyl nitrate to solutions with fixed pH 8.3 and with Ca and total carbonate concentrations fixed at the concentrations of those in calcite-saturated solutions of pH = 8.3 and $P(CO_2) = 10^{-3.5}$ bar.

co-added carbonate. Sharp diffraction lines were observed only for the calcite sorbent. In the sample for which U(VI) was added without CO_3, broad, diffuse maxima were evident in the XRD pattern, indicating the presence of an X-ray amorphous phase. Broad maxima centered at ~11° and ~28° two-theta (Cu $K\alpha$) and a broader feature at higher angles cannot be readily associated with any unique phase. Previous authors have noted that a wide variety uranyl hydroxide phases can be synthesized at ambient conditions (e.g., schoepite, metaschoepite), some of which may be poorly crystalline and variably hydrated (e.g., Finch et al., 1997). The broad maxima at 11° and 28° two-theta show only a weak correspondence with the strongest diffractions for schoepite and metaschoepite. However, a similar weak correspondence is also observed for the calcium-containing uranyl hydroxide becquerelite [$Ca(UO_2)_6O_4(OH)_6$•$8H_2O$] and the uranyl carbonate hydrate joliotite (UO_2CO_3•$2H_2O$), as well as several synthetic calcium uranyl carbonate hydrates. Because these phases share broad similarities in their XRD patterns and because the precipitate in our sample is X-ray amorphous, we cannot uniquely identify the precipitate, which could consist of multiple phases and/or solid solutions. The XRD pattern of the sample where carbonate was co-added does not show the same broad, diffuse maxima, but does show weak peaks at 18° and 34.3° two-theta (Fig. 4, inset). These do not correspond to any of the phases considered above. The extent of precipitation was much higher in the sample without co-added carbonate, indicating that co-addition of carbonate stabilizes U(VI) against precipitation, consistent with the speciation calculations presented above, and the EXAFS data presented below. The XRD results indicate that not only the extent of precipitation, but also the final U(VI) precipitate formed is influenced by the co-addition of carbonate.

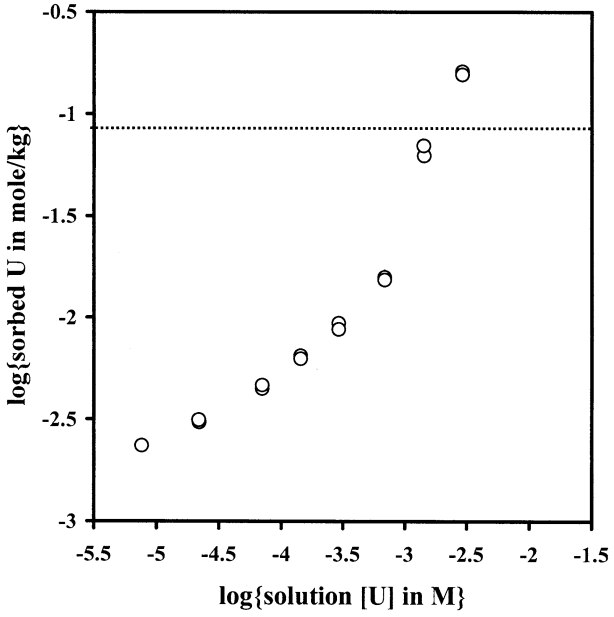

Fig. 3. Adsorption isotherm of U(VI) sorption to calcite in preequilibrated solutions at pH 8.3 and $P(CO_2) = 10^{-3.5}$ bar. The dashed vertical line indicates the concentration of Ca surface sites at the calcite surface.

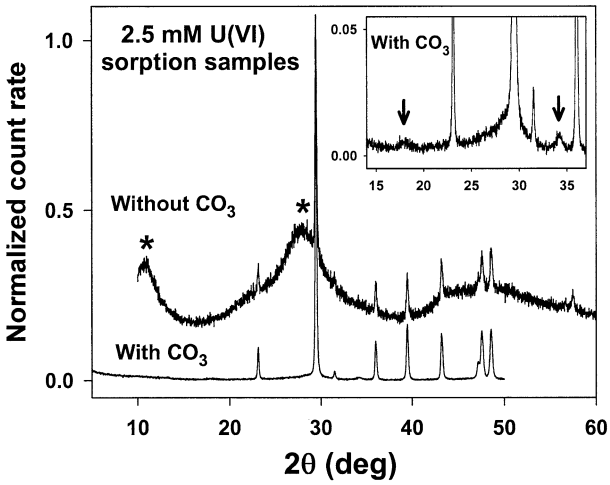

Fig. 4. Powder X-ray diffraction data (Cu $K\alpha$) for dried calcite sorption samples reacted with 2.5 mM U(VI). In the bottom scan U(VI) was added as a uranyl carbonate solution (with carbonate). In the top scan, U(VI) was added as a uranyl nitrate solution (i.e., without carbonate). Count rates were normalized for comparison, and scans are offset for clarity. The inset is an enlarged version of the bottom spectrum. Arrows and asterixes denote peaks indicative of U(VI) precipitates.

4.4. EXAFS Fit Results

The raw and fitted k^3-weighted χ spectra of the samples analyzed by EXAFS are shown in Figure 5a, and the radial structure functions (RSFs, Fourier transform magnitudes) of these spectra are shown in Figure 5b. The data for the samples reacted at low [U] (<500 μM) all resemble the spectrum of the aqueous triscarbonate complex, except that the contribution of the equatorial shell in the RSFs of these samples is lower in magnitude than that of the aqueous triscarbonate complex and

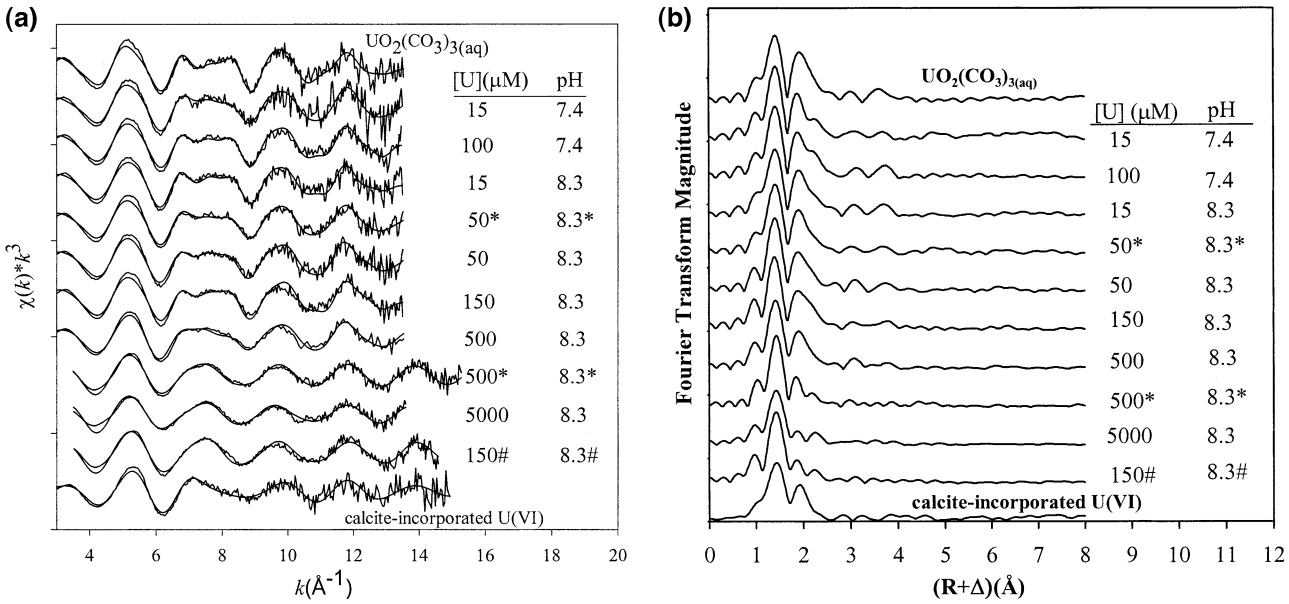

Fig. 5. (a) Raw and fitted k^3-weighted χ functions for U(VI)-sorption samples and reference samples, and (b) corresponding Fourier transform magnitudes. * indicates samples without co-added CO_3; # indicates dried sample.

has a shoulder on the high-R side. This indicates slight splitting in the equatorial shell of the adsorbed U(VI) complexes, or possibly the presence of a mixture of U(VI) species that have different equatorial O shell coordinations at the calcite surface. Due to the similarity in the EXAFS data of the uranyl triscarbonate complex and those of the low-loading U(VI) adsorption complexes at the calcite surface, the sorption sample fits presented in Figure 5 were generated using the same theoretical paths as for the triscarbonate complex. In addition to the axial and equatorial O shells, these included scattering from a C shell at ~2.90 Å, a multiple-scattering (MS) U-$O_{axial(1)}$-U-$O_{axial(2)}$ path with a radial distance approximately twice that of the U-O_{axial} distance, another O shell at 4.1–4.2 Å (O_{distal}), and the linear U- O_{distal} -C MS path with R = 4.1–4.2 Å. FEFF7 calculations indicated the importance of another MS contribution at ~4 Å in the U(VI) triscarbonate complex, U-C-*O*-C scattering, with an amplitude approximately half that of the U-*O*-C MS path. To avoid physically unrealistic fitting parameters as a result of fitting a number of overlapping scattering paths to a weak signal, inclusion of this MS path in the fitting procedure required constraining its distance to be the same as the distance of the U-O path (as it theoretically should be). Inclusion of this path, however, did not improve the fit quality; therefore, fitting was done using only the single scattering U-O_{distal} and the MS U- O_{distal} -C MS paths without constraints except for fixed N values. While using these scattering paths yielded reasonable fits of the experimental spectra, we cannot entirely rule out the possibility of Ca and/or U neighbors in the coordination sphere of sorbed U. Coordination of the triscarbonate complex to Ca^{2+} in a CO_3-bridging coordination, as observed in liebigite and aqueous $Ca_2UO_2(CO_3)_3$, yields a U-Ca distance of approximately 4 Å (Bernhard et al., 2001). Therefore, U-Ca back-scattering, if present, would be obscured by U-O_{distal} scattering at ~4.14 Å, and multiple scattering at a similar distance. We were able to fit a small Ca contribution at approximately 4 Å, but this did not improve the fit due to the overlap with these other shells; exclusion of U-Ca amplitude could be compensated by slight changes in the U-O_{distal} and MS amplitudes. This was also observed by Bernhard et al. (1996, 2001) in fitting EXAFS data of the aqueous $Ca_2UO_2(CO_3)_3$ complex. Difficulties in determining U-outer shell scattering at ambient temperatures have been noted in the literature (Thompson et al., 1997).

While the fits presented in Figure 5 used a single equatorial U-O scattering path for the low [U] sorption samples, it was also possible to get a good fit using split shells, as shown in Figure 6. Although the RSF seems better described by using a split equatorial shell, there is no discernible improvement in the χ description of the data, which is why the majority of the samples were fitted with a single equatorial oxygen shell.

The multimeric uranyl triscarbonate complexes characterized by Allen et al. (1995) have slightly split equatorial O shells similar to our sorption samples, and U-U distances of approximately 5 Å. The RSFs of our sorption samples do not show features in this region above noise level, but it should be noted that the U-U scattering in the study by Allen et al. (1995) shows up in the RSFs as quite subtle features. The EXAFS data of the low [U] sorption samples are, therefore, consistent with the presence of uranyl triscarbonate-like complexes at the calcite surface, but do not allow for identification of the exact coordination (i.e., inner- or outer-sphere complexes, monomers or multimers) of these complexes. The slight distortion in the equatorial O shell, suggestive of splitting, may be due to binding to surface Ca atoms or due to polymerization. The presence of a mixture of U(VI) sorption products with different equatorial O shells cannot be excluded. It should be noted that there is a consistent decrease in bond distance of the outer shell in the EXAFS data (U-O_{dist} shell in Table 1) with increasing U(VI) loading (at [U] $<$500 μM), suggesting that more than one triscarbonate-like complex could be present. The EXAFS

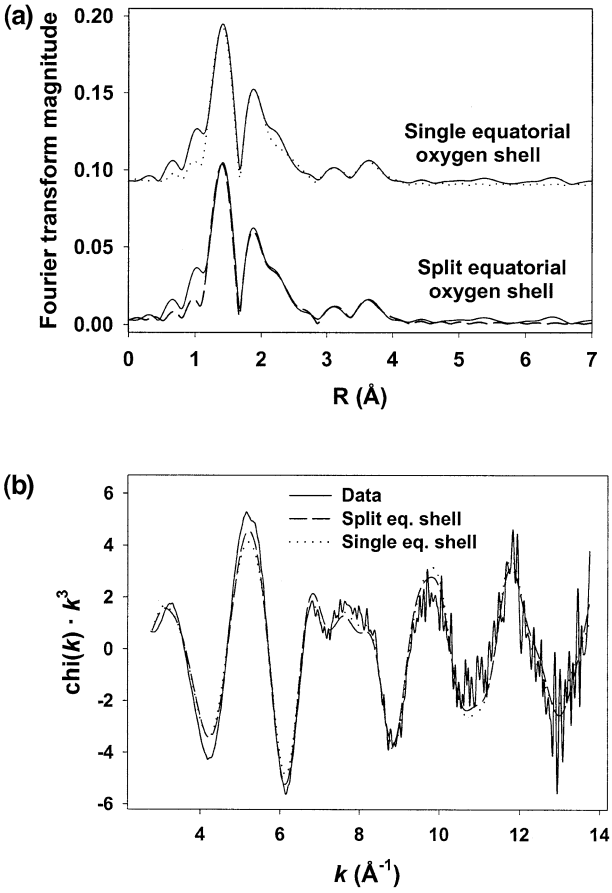

Fig. 6. (a) Raw and fitted Fourier transform magnitudes using a single and a split equatorial O shell of the U(VI)-calcite sorption sample reacted at pH 8.3 and [U(VI)] = 150 μM; (b) corresponding χ fits compared to the experimental spectrum.

of the low [U(VI)] sorption samples also differ from U(VI) coprecipitated with bulk polycrystalline calcite (Fig. 7), which was previously characterized (Reeder et al., 2000, 2001).

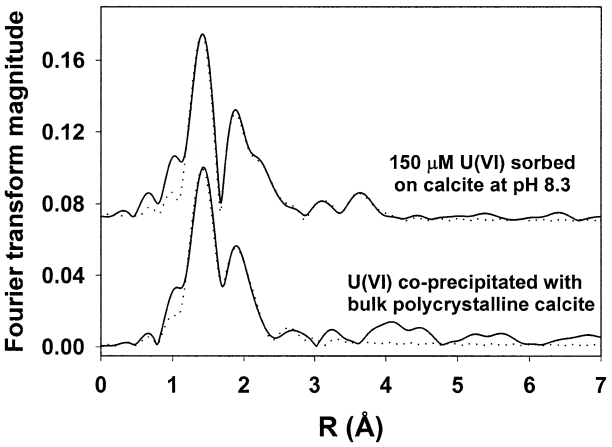

Fig. 7. Comparison of Fourier transform magnitudes for U(VI) adsorbed at the calcite surface and U(VI) incorporated into bulk polycrystalline calcite.

The sample reacted at high [U] (5 mM) shows a distinctly split equatorial O shell, with oxygens at 2.26 Å and 2.46 Å. Five shells were used to fit this spectrum: O_{axial}, two O_{eq}, MS at twice the distance of the U-O_{axial} path, and U-C (Table 1), which resulted in a reasonable fit of the experimental spectrum (Fig. 5). Based on the speciation calculations (Fig. 1) and the isotherm data (Fig. 3) presented above, the most likely cause for the difference in U coordination relative to the low [U] samples is the formation of uranyl (hydroxide/carbonato) precipitates. No U-U scattering was identified, however, suggesting that U present in the precipitates formed does not have a close U neighbor or, if it does, one with a single well-defined local structure, but rather exhibits a range of U-U distances. This may be due to dispersion in U-U distances within a "single" precipitate phase (as observed for Th-hydroxide; Rothe et al., 2002; also see Thompson et al. (1997) for a discussion of U-U backscattering peaks at room temperature versus 10K), and/or the formation of a multi-phase precipitate, e.g., precipitates with different degrees of hydration. Speciation

Table 1. EXAFS fit parameters for uranyl sorbed by calcite and reference samples.

		U-O_{axial}			U-O_{eq1}			U-O_{eq2}			U-C			MS 1			U-O_{distal}			MS 2		
[U](uM)	pH	N	R (Å)	σ^2 (Å^2)	N	R (Å)	σ^2 (Å^2)	N	R (Å)	σ^2 (Å^2)	N	R (Å)	σ^2 (Å^2)	N	R (Å)	σ^2 (Å^2)	N	R (Å)	σ^2 (Å^2)	N	R (Å)	σ^2 (Å^2)
$UO_2(CO_3)_{3(aq)}^{4-}$		2	1.80	0.001	6	2.42	0.005	—	—	—	3	2.87	0.001	2	3.59	0.002	3	4.26	0.004	6	4.12	0.004
15	7.4	2	1.80	0.001	6	2.39	0.008	—	—	—	3	2.90	0.002	2	3.59	0.001	3	4.22	0.008	6	4.16	0.008
100	7.4	2	1.80	0.001	6	2.41	0.007	—	—	—	3	2.89	0.002	2	3.61	0.001	3	4.14	0.003	6	4.18	0.003
15	8.3	2	1.80	0.001	6	2.41	0.007	—	—	—	3	2.90	0.001	2	3.61	0.002	3	4.21	0.006	6	4.16	0.006
50*	8.3*	2	1.80	0.001	6	2.40	0.008	—	—	—	3	2.89	0.003	2	3.60	0.002	3	4.17	0.007	6	4.18	0.007
50	8.3	2	1.80	0.001	6	2.41	0.008	—	—	—	3	2.93	0.003	2	3.63	0.001	3	4.15	0.004	6	4.20	0.004
150	8.3	2	1.79	0.001	6	2.41	0.008	—	—	—	3	2.90	0.002	2	3.60	0.002	3	4.12	0.002	6	4.18	0.002
500	8.3	2	1.81	0.001	6	2.39	0.010	—	—	—	3	2.92	0.005	2	3.64	0.001	3	3.98	0.009	6	4.15	0.009
500*	8.3*	2	1.82	0.001	3	2.25	0.009	3	2.45	0.011	—	—	—	2	3.66	0.003	—	—	—	—	—	—
5000	8.3	2	1.82	0.002	3	2.25	0.010	3	2.53	0.010	—	—	—	2	3.65	0.004	—	—	—	—	—	—
150[#]	8.3[#]	2	1.81	0.001	3	2.22	0.008	3	2.45	0.012	—	—	—	2	3.63	0.002	—	—	—	—	—	—
U:calcite		2	1.80	0.002	5	2.34	0.008	—	—	—	3	2.89	0.007	2	3.56	0.005	—	—	—	—	—	—

Coordination number N was fixed to values in triscarbonate complex. Errors for R are ± 0.01 Å for first and second shells, and 0.02–0.04 Å for more distant shells. Errors for the Debye-Waller factors are estimated at ± 0.001–0.002 Å^2.

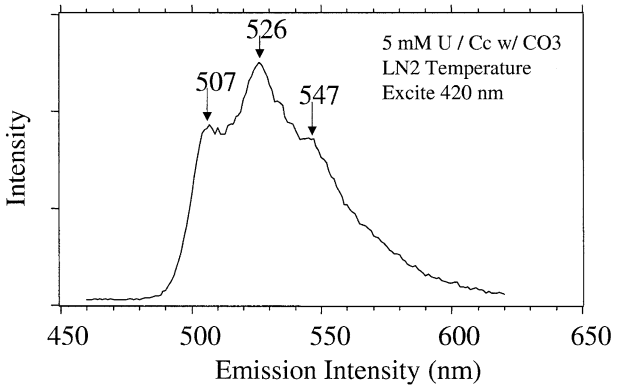

Fig. 8. Luminescence spectrum of moist calcite paste exposed to a 5 mM uranyl solution under atmospheric CO_2.

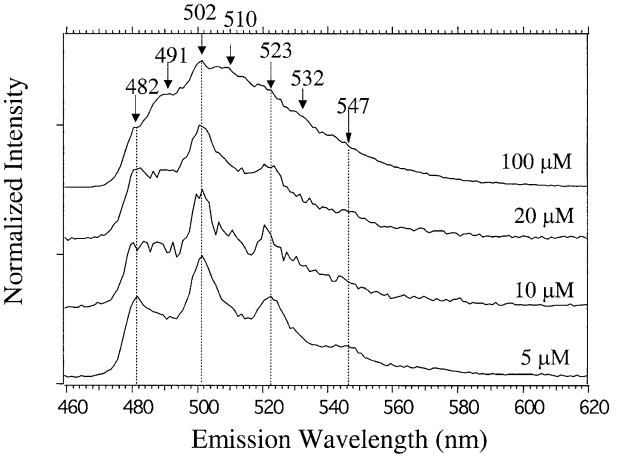

Fig. 9. Normalized luminescence spectra of moist calcite pastes exposed to uranyl solutions of different concentrations under atmospheric CO_2.

calculations indicated oversaturation with respect to uranyl hydroxides (Fig. 2). However, quite likely the precipitates that formed are not pure phases, but contain Ca and CO_3 as well, adding to their complexity.

There is no discernable difference in the EXAFS spectra of samples reacted at pH 8.3 and pH 7.4 (Fig. 5 and Table 1), suggesting that the same mode of U(VI) uptake occurs at both pH conditions. This is consistent with the speciation calculations, which indicated that the U(VI) solution speciation is essentially the same at these pH values under the reaction conditions employed here. The co-addition of carbonate does not have a noticeable effect on U(VI) surface speciation at low (50 μM) [U]. At [U] = 500 μM, however, there is an obvious effect: the sample with co-added carbonate shows the same triscarbonate surface complex that is also observed at lower [U], whereas the EXAFS data of the sample without co-added carbonate are similar to the high [U] sample, where precipitation is thought to occur (Fig. 5 and Table 1). Introducing U(VI) as the triscarbonate complex to the calcite suspensions at high U(VI) concentrations is found to stabilize added U(VI) against the formation of uranyl precipitates, consistent with the speciation calculations presented above.

4.5. Luminescence Results

The luminescence spectra from the calcite-sorbed U(VI) samples are observed to change as [U] in the overlying solution (and therefore the U loading at the calcite surface) is changed (Figs. 8 and 9). At high [U] (Fig. 8), the spectrum is relatively unstructured and centered at 526 nm (19000 cm^{-1}). From the previous discussion, uranyl hydroxide/carbonate precipitates are expected at these concentrations, and indeed the spectrum shown in Figure 8 is consistent with the luminescence spectra of uranyl hydroxide precipitates shown in the literature (Morris et al., 1996; Geipel et al., 1997; Duff et al., 2000). The non-exponential excited state lifetime (double exponential fit with 135 and 380 μs lifetimes) indicates that the precipitate is not a pure phase, which is not surprising considering the variability in hydration of uranyl hydroxide/schoepite precipitates (Finch et al., 1998). The presence of multi-phase precipitates may result in a multitude of local coordination environments around precipitated U(VI), and may therefore at least partially explain why no U-U scattering was observed in the EXAFS spectra of the high concentration samples with U precipitation.

In contrast, the spectra at low [U(VI)] ($\leq$100 μM, Fig. 9) are distinctly blue-shifted from the uranyl hydroxide precipitates (Fig. 8). Based on the isotherm data and EXAFS results presented above, it is likely that this new set of luminescence spectra represents the truly adsorbed uranyl species. Increasing structure as [U] decreases from 100 μM to 5 μM, as well as the nonexponential lifetimes of the higher [U] samples in this set, imply that more than one species is present throughout the series. A double exponential fit to the luminescence decay spectrum of the 10 μM sample yielded lifetimes of 125 $\pm$ 30 μs and 580 $\pm$ 240 μs (420 nm excitation, 509 nm detection), allowing for time-resolved decomposition of the spectra (Fig. 10). The gated spectra collect the emitted light only at certain times after the excitation flash: from delay times 50 to 100 μs after the excitation flash for the short gate and from delay times 700 to 1500 μs after the flash for the delayed gate. The delayed gate brings out the vibronic structure that is apparent at the

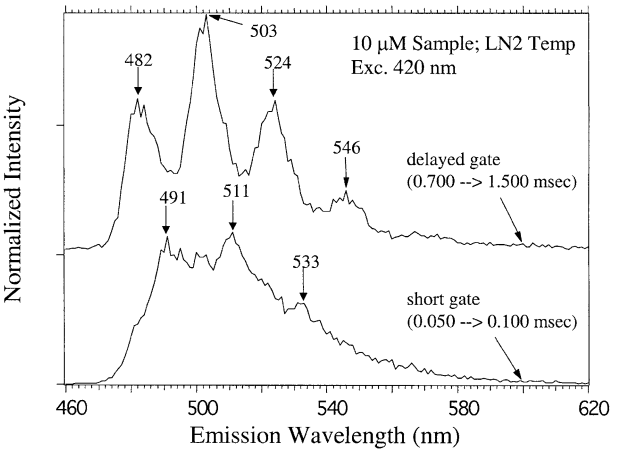

Fig. 10. Time-resolved luminescence spectra of a moist calcite paste exposed to a 10 μM uranyl solution under atmospheric CO_2.

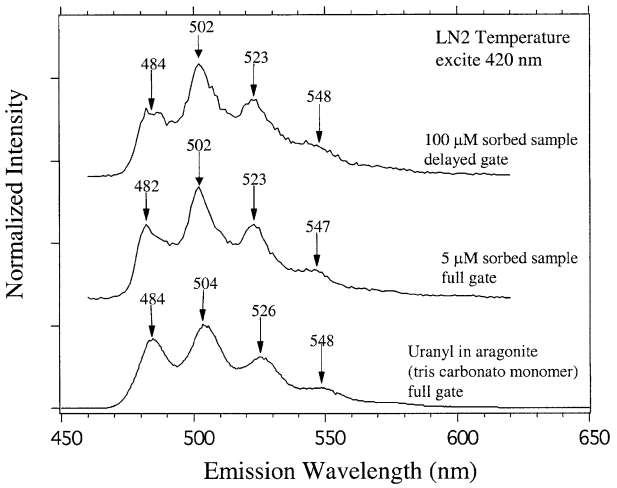

Fig. 11. Luminescence spectra of uranyl sorbed on calcite compared to that of uranyl incorporated into aragonite.

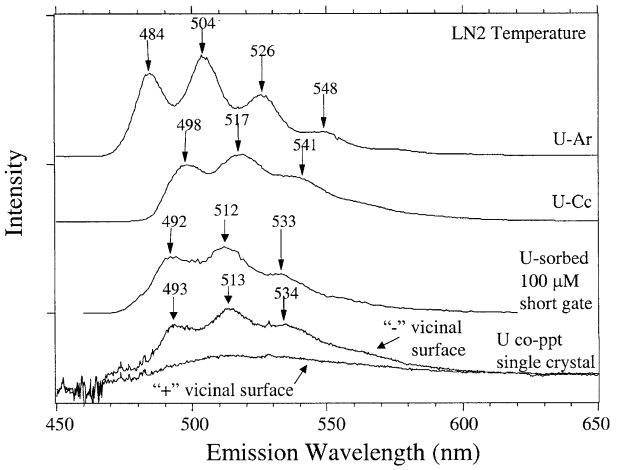

Fig. 12. Luminescence spectra of uranyl incorporated into bulk aragonite, incorporated into bulk calcite, sorbed on calcite using a short gate, and incorporated into the (10$\bar{1}$4) face of a single calcite crystal.

lowest concentration spectrum in Figure 9 from the 5 μM sample. The increased resolution with gating applies even for the 100 μM sample (Figs. 10 and 11), which has the least amount of resolution when the full decay curve is collected for the spectrum (Fig. 9). Different peaks are apparent in the spectrum with the short gate. Therefore, there are at least two detectable species of uranyl sorbing onto the calcite. The first is present throughout the series and dominates at the lowest loading level (5 μM). This species has a longer lifetime than the second species, which is seen to "grow-in" as [U] increases. The appearance of this second species as [U] is increased makes the non-gated spectra at higher concentrations appear less resolved due to the addition of both spectra.

The spectra for the longer-lived species that is observed most readily at lower [U] can be compared to luminescence spectra of known uranyl species (Fig. 11). The vibronically resolved peaks match up well with the peaks from uranyl coprecipitated with aragonite and that from the mineral liebigite, which are from the species $Ca_2UO_2(CO_3)_3$ (Reeder et al., 2000, 2001). This species was also shown to have a 590 μs lifetime in the aragonite matrix at 77 K (Reeder et al., 2000). Therefore, at the lowest uranyl loadings onto calcite, the sorbed species is the calcium uranyl triscarbonate species.

The identification of the second (short-gate) U(VI) surface species, growing in with increasing [U], is not trivial, as comparison of the spectrum for this second species to spectra of known uranyl carbonate complexes is problematic. There is considerable literature regarding the luminescence quenching by carbonate groups bound to uranyl (Saini et al., 1989; Meinrath, 1997), and the effect of calcium cations to counter this effect has just recently been recognized (Bernhard et al., 1996; Geipel et al., 1997). The second spectrum found here does not match that of the monocarbonate UO_2CO_3 in either the aqueous phase (Meinrath, 1997) or solid phase (rutherfordine, Reeder et al., 2000), nor does it match the spectrum for the uranyl carbonate trimer $[C(NH_2)_3]_6[(UO_2)_3(CO_3)_6]\cdot 6.5H_2O$ (unpublished data). Spectra are not available for the monomeric biscarbonate species $[UO_2(CO_3)_2]^{2-}$ (Meinrath, 1997) or the dimeric hemicarbonate $[(UO_2)_2CO_3(OH)_3]^-$ (Saini et al., 1989), both of which are potentially available in solution (Fig. 1). We note that an interesting comparison, however, can be made between the luminescence spectrum of this second species and that for uranyl coprecipitated at the (10$\bar{1}$4) surface of calcite single crystals. The spectrum of uranyl coprecipitated at the "-" vicinal surface of a (10$\bar{1}$4) face of a calcite single crystal in Figure 12 (bottom spectrum) was obtained using a spatially resolved fluorescence method. Reeder et al. (2001) showed that incorporation of uranyl is strongly favored at the growth steps that compose "-" vicinal surfaces, resulting in a heterogeneous distribution within the bulk crystal. We note that the luminescence spectrum of the second sorbed uranyl species (appearing at higher [U]) bears a strong resemblance to this spectrum for uranyl coprecipitated within a portion of the single calcite crystal. Furthermore, the luminescence spectrum for the second species appears at an energy that is intermediate to that for the triscarbonate species found in aragonite and uranyl incorporated into bulk polycrystalline calcite. In synthetic polycrystalline calcite, the equatorial coordination number changed from six (three bidentate CO_3) in $[UO_2(CO_3)_3]^{4-}$ to five, as CO_3 groups were forced to twist around to conform to the calcite structure (Reeder et al., 2000, 2001). Decreasing the equatorial coordination number allowed the U-O_{eq} distance to shift from 2.43 to 2.33 Å. It also shortened the excited state lifetime to 125 μs (Reeder et al., 2000), comparable to the 125 μs measured for the short component of the second sorbed species here.

5. DISCUSSION

The EXAFS and luminescence data for the high U(VI) loading samples ([U] = 2.5 and 5 mM) indicate the formation of precipitates in these samples, which is in agreement with the speciation calculations. The XRD and luminescence data indicate that the precipitates are X-ray amorphous and possibly multi-phase, but may have similarities to uranyl carbonate-hydroxide and/or schoepite-like phases. Carroll et al. (1992)

and Geipel et al. (1997) also presented evidence for the formation of U(VI) precipitates at high U loadings in calcite-containing systems. Our findings indicate that precipitate formation is enhanced when UO_2^{2+} is introduced to a system lacking sufficient dissolved carbonate to allow for uranyl carbonate complexation, consistent with speciation calculations. Additionally, the XRD results suggest that co-addition of carbonate also influences the type of U(VI) precipitates that form.

For the lower U(VI) loading samples, the EXAFS data are consistent with the dominant formation of a uranyl triscarbonate complex with a slightly distorted equatorial shell. The luminescence data, on the other hand, indicate the formation of two U(VI) species in this lower loading region, with a calcium uranyl triscarbonate complex dominating at the lowest loadings, and, as loading increases, the increased formation of another U(VI) species. The luminescence spectrum of this latter species is intermediate between the triscarbonate species found at the lowest loadings and the uranyl carbonate incorporated into bulk polycrystalline calcite, which suggest that it may be from another uranyl triscarbonato-like species. Furthermore, this latter spectrum resembles that of uranyl selectively incorporated into the $(10\bar{1}4)$ "-" vicinal surface of a calcite single crystal. The steric restraints imposed by incorporation only into the "-" face of the single crystal constrain the possibilities for the identity of the triscarbonato-like uranyl species.

The apparent discrepancy between the EXAFS and luminescence data in the low [U] range (i.e., a change in U(VI) surface speciation with loading based on luminescence results, but only a subtle change in EXAFS in the U-O4 shell results at different loadings) may be explained by a number of factors. First of all, the quantum luminescence yields for these species are not known; therefore, the relative proportions of the different species found in the luminescence results cannot be estimated with confidence. If the yield for one species is much higher than for the other, this species may strongly influence the luminescence data even at relatively low abundance. EXAFS weight-averages over the contributions from all absorbers. It is possible that one of the U(VI) sorption species has a much higher luminescence yield than the other, but is not observed in the EXAFS spectra due to its low abundance.

Perhaps a more likely explanation is that the difference in the local coordination of these two species observed in the luminescence experiments is too subtle to be discerned by EXAFS. The second U(VI) species observed by luminescence at intermediate [U] has a luminescence spectrum that is intermediate between that of the triscarbonate species found at the lowest loadings and the uranyl incorporated into synthetic polycrystalline calcite. Uranyl incorporated into the calcite bulk has a five-fold equatorial shell with an average $U\text{-}O_{eq}$ distance of 2.33 Å (Reeder et al., 2000; Table 1), whereas uranyl incorporated into aragonite has a sixfold equatorial O coordination and retains the triscarbonate complex symmetry (Reeder et al., 2000, 2001). The intermediate species forming at the calcite surface at higher loadings (but below saturation with respect to uranyl hydroxides) is not likely to be uranyl sorbed in a monodentate fashion to carbonate on the calcite surface to form a similar 5-coordinate species. Such a coordination change would result in markedly different $U\text{-}O_{eq}$ bond lengths than observed. However, it is possible that this species is a distorted triscarbonate-like complex, perhaps with slightly twisted CO_3 coordinated to Ca surface atoms, or possibly incorporated in the near surface region. Alternatively, both sorbed species could be triscarbonate species with nearest-neighbor calciums in different positions. In all of these cases, the sorption complex has significant triscarbonate complex character with a (slightly) split equatorial O shell, consistent with the EXAFS data. Assuming that the EXAFS spectra of the samples reacted at 150 and 500 μM are dominated by this second complex, it is clear from Figures 5a and 5b that it strongly resembles that of aqueous $UO_2(CO_3)_3^{4-}$, and would therefore be difficult to distinguish from the triscarbonate sorption complex dominating at low-surface coverage, as determined from the luminescence results.

The relatively low degree of U(VI) adsorption evident from the adsorption isotherm (Fig. 3) suggests that the interaction of the triscarbonate U(VI) adsorption complexes with the calcite surface is limited. The onset of U(VI) precipitation occurs at concentrations far below surface site saturation (indicated by the dashed line in Figure 3), and the triscarbonate adsorption complexes transform into U(VI) precipitates upon sample drying (at room temperature), as evident from the spectrum of the dried sample in Figure 5. The surface site occupancy in this sample is estimated to be only 7%; yet, the U(VI) adsorption complexes in this sample apparently possessed sufficient mobility and affinity for precipitation to occur when the sample dried out. Fits to the EXAFS data of this sample were done using the same shells as for the high-loading samples showing precipitation (Table 1). A slight improvement in the fit was observed when including a U-C shell at 2.9 Å (not shown), suggesting that part of the carbonate groups associated with the triscarbonate sorption complexes were incorporated in the precipitates formed upon drying. The weak interaction of the U(VI) triscarbonate complexes with the calcite surface may be due to the strong $U\text{-}CO_3$ complexation in solution, which makes coordination to surface Ca^{2+} atoms relatively unfavorable, especially when compared to the competitive coordination of uncomplexed CO_3^{2-} anions.

6. CONCLUDING REMARKS

The results from EXAFS and luminescence characterization of U(VI) sorption complexes formed in air-equilibrated ($P(CO_2) = 10^{-3.5}$ bar) calcite suspensions of pH 8.3 suggest a complicated sequence of interactions. At solution [U] >500 μM, the formation of complex uranyl hydroxide- and carbonate-containing precipitates is observed, whereas at lower concentrations mononuclear triscarbonate-like U(VI) adsorption complexes form at the calcite-water interface, consistent with isotherm data and speciation calculations. The EXAFS data indicate a strongly split equatorial O shell for the U(VI) precipitates, whereas the U(VI) adsorption complexes have a weakly split equatorial shell, possibly indicating that the adsorption complexes are bound in an inner-sphere fashion at the calcite surface, although no Ca scattering could be isolated. The luminescence data indicate the presence of at least two adsorption complexes that change proportion with U(VI) loading. The species dominating at low-surface coverage is a calcium uranyl triscarbonate complex similar in structure to uranium in liebigite. A second species is observed at higher surface loadings with a luminescence spectrum that is intermediate between the triscarbonate species found at the lowest loadings and uranyl incorporated into bulk polycrystalline calcite. Combined,

the EXAFS and luminescence data indicate the adsorption complexes formed at the calcite surface are triscarbonate-like U(VI) complexes, with a change in interaction with the surface as the surface loading increases.

The complexity that is evident when uranyl species interact at the calcite-water interface in controlled experiments suggests the potential for equal or greater complexity in natural systems. The presence of multiple uranyl species suggests that kinetic uptake behavior could exhibit multiple trends, and retention behavior of U(VI) sorbed by calcite may exhibit multi-phase character. It must be considered, however, that the relatively short duration of the sorption experiments described here may not necessarily capture any effects associated with sample aging. For example, Kelly et al. (2003) found a local coordination of U(VI) coprecipitated with natural calcite from a speleothem sample that differs from the synthetic U(VI):calcite coprecipitation of our previous work (Reeder et al., 2000, 2001). Presumably, factors that influence the process, including time, result in the different solid speciation. Similarly, differences in environmental parameters between laboratory and natural conditions, as well as among different natural conditions, may result in variability in the solid speciation of U(VI) sorbed with calcite.

Acknowledgments—This work was supported by the Center for Environmental Molecular Science through NSF grant CHE0221934 and by DOE grant DE-FG07–99ER15013. We thank J. Linton, M. Beno, and the BESSRC CAT at the APS for assistance with data collection. We also thank L. Soderholm and S. Skanthakumar for use of the Actinide Facility at Argonne National Laboratory for sample handling and transport. CDT and DEM were supported by the LANL Laboratory Directed Research and Development Program. KDR was supported by the LANL Frederick Reines Postdoctoral Fellowship. Comments by K. Nagy, N. Sturchio, and two anonymous reviewers improved the manuscript.

Associate editor: K. L. Nagy

REFERENCES

Allen P. G., Bucher J. J., Clark D. L., Edelstein N. M., Ekberg S. A., Gohdes J. W., Hudson E. A., Kaltsoyannis N., Lukens W. W., Neu M. P., Palmer P. D., Reich T., Shuh D. K., Tait C. D., and Zwick B. D. (1995) Multinuclear NMR, Raman, EXAFS, and X-ray-diffraction studies of uranyl carbonate complexes in near-neutral aqueous solution. X-ray structure of $[C(NH_2)_3]_6[(UO_2)_3(CO_3)_6] \cdot 6.5H_2O$. *Inorg. Chem.* **34,** 4797–4807.

Ankudinov A. L. and Rehr J. J. (1997) Relativistic Spin-dependent X-ray Absorption Theory. *Phys. Rev. B.* **56,** R1712–R1715.

Bargar J. R., Reitmeyer R., and Davis J. A. (1999) Spectroscopic confirmation of uranium(VI)- carbonato adsorption complexes on hematite. *Env. Sci. Technol.* **33,** 2481–2484.

Bargar J. R., Reitmeyer R., Lenhart J. J., and Davis J. A. (2000) Characterization of U(VI)- carbonato ternary complexes on hematite: EXAFS and electrophoretic mobility measurements. *Geochim. Cosmochim. Acta* **64,** 2737–2749.

Bernhard G., Geipel G., Brendler V., and Nitsche H. (1996) Speciation of uranium in seepage waters of a mine tailing pile studied by time-resolved laser-induced fluorescence spectroscopy (TRLFS). *Radiochim. Acta* **74,** 87–91.

Bernhard G., Geipel G., Reich T., Brendler V., Amayri S., and Nitsche H. (2001) Uranyl(VI) carbonate complex formation. Validation of the $Ca_2UO_2(CO_3)_3$(aq.) species. *Radiochim. Acta* **89,** 511–518.

Carroll S. A. and Bruno J. (1991) Mineral-solution interactions in the U(VI)-CO_2-H_2O system. *Radiochim. Acta* **52/53,** 187–193.

Carroll S. A., Bruno J., Petit J-C., and Dran J-C. (1992) Interaction of U(VI), Nd, and Th(IV) at the calcite-solution interface. *Radiochim. Acta* **58/59,** 245–252.

Clark D. L., Conradson S. D., Donohoe R. J., Keogh D. W., Morris D. E., Palmer P. D., Rogers R. D., and Tait C. D. (1999) Chemical speciation of the uranyl ion under highly alkaline conditions. Synthesis, structures, and oxo ligand exchange dynamics. *Inorg. Chem.* **38,** 1456–1466.

Duff M. C., Morris D. E., Hunter D. B., and Bertsch P. M. (2000) Spectroscopic characterization of uranium in evaporative basin sediments. *Geochim. Cosmochim. Acta* **64,** 1535–1550.

Fenter P., Geissbuehler P., DiMasi E., Srajer G., Sorensen L. B., and Sturchio N. C. (2000) Surface speciation of calcite observed in situ by high-resolution X-ray reflectivity. *Geochim. Cosmochim. Acta* **64,** 1221–1228.

Finch R. J., Hawthorne F. C., Miller M. L., and Ewing R. C. (1997) Distinguishing among schoepite and related minerals by x-ray diffraction. *Powder Diffraction* **12,** 230–238.

Finch R. J., Hawthorne F. C., and Ewing R. C. (1998) Crystallographic relations among schoepite, metaschoepite, and dehydrated schoepite. *Can. Mineral.* **36,** 831–845.

Geipel G., Reich T., Brendler V., Bernhard G., and Nitsche H. (1997) Laser and X-ray spectroscopic studies of uranium-calcite interface phenomena. *J. Nuclear Mater.* **248,** 408–411.

Grenthe I., Fuger J., Konings R., Lemire R. J., Muller A. B., Nguyen-Trung C. and Wanner J. (1992) The Chemical Thermodynamics of Uranium. Elsevier.

Hsi C-K. D. and Langmuir D. (1985) Adsorption of uranyl onto ferric oxyhydroxides: Application of the surface complexation site-binding model. *Geochim. Cosmochim. Acta* **49,** 1931–1941.

Kalmykov S. N. and Choppin G. R. (2000) Mixed $Ca^{2+}/UO_2^{2+}/CO_3^{2-}$ complex formation at different ionic strengths. *Radiochim. Acta* **88,** 603–606.

Kaplan D. I., Gervais T. L., and Krupka K. M. (1998) Uranium(VI) sorption to sediments under high pH and ionic strength conditions. *Radiochim. Acta* **80,** 201–211.

Kelly S. D., Newville M. G., Cheng L., Kemner K. M., Sutton S. R., Fenter P., Sturchio N. C., and Spotl C. (2003) Uranyl incorporation in natural calcite. *Env. Sci. Tech.* **37,** 1284–1287.

Langmuir D. (1997) Aqueous Environmental Chemistry. Prentice-Hall.

Lenhart J. J. and Honeyman B. D. (1999) Uranium(VI) sorption to hematite in the presence of humic acid. *Geochim. Cosmochim. Acta* **63,** 2891–2901.

McKinley J. P., Zachara J. M., Smith S. C., and Turner G. D. (1995) The influence of hydrolysis and multiple site-binding reactions on adsorption of U(VI) to montmorillonite. *Clays Clay Minerals* **43,** 586–598.

Meinrath G. (1997) Uranium(VI) speciation by spectroscopy. *J. Radioanal. Nucl. Chem.* **224,** 119–126.

Morris D. E., Chisholm-Brause C. J., Barr M. E., Conradson S. D., and Eller P. G. (1994) Optical spectroscopic studies of the sorption of UO_2^{2+} species on a reference smectite. *Geochim. Cosmochim. Acta* **58,** 3613–3623.

Morris D. E., Allen P. G., Berg J. M., Chisholm-Brause C. J., Conradson S. D., Donohoe R. J., Hess N. J., Musgrave J. A., and Tait C. D. (1996) Speciation of uranium in Fernald soils by molecular spectroscopic methods: Characterization of untreated soils. *Env. Sci. Tech.* **30,** 2322–2331.

Morse J. W., Shanbhag P. M., Saito A., and Choppin G. R. (1984) Interaction of uranyl ions in carbonate media. *Chem. Geol.* **42,** 85–99.

Pabalan R. T., Turner D. R., Bertetti F. P. and Prikryl J. D. (1998) Uranium VI sorption onto selected mineral surfaces. Key geochemical parameters. In *Adsorption of Metals by Geomedia* (ed. E. Jenne), pp. 99-130, Academic Press.

Paquette J. and Reeder R. J. (1995) Relationship between surface structure, growth mechanism, and trace element incorporation in calcite. *Geochim. Cosmochim. Acta* **59,** 735–749.

Parkhurst D. L. and Appelo C. A. J. (1999) User's guide to PHREEQC (Version 2)—A computer program for speciation, batch-reaction, one-dimensional transport and inverse geochemical calculations. *U.S. Geological Survey Water-Resources Investigations Report* **99–4259** 310 p.

Payne T. E., Lumpkin G. R., and Waite T. D. (1998) Uranium VI adsorption on model minerals. In *Adsorption of Metals by Geomedia* (ed. E. Jenne), pp. 75–97. Academic Press.

Reeder R. J. (1996) Interaction of divalent cobalt, zinc, cadmium, and barium with the calcite surface during layer growth. *Geochim. Cosmoshim. Acta* **60,** 1543–1552.

Reeder R. J., Nugent M., Lamble G. M., Tait C. D., and Morris D. E. (2000) Uranyl incorporation into calcite and aragonite: XAFS and luminescence studies. *Env. Sci. Tech.* **34,** 638–644.

Reeder R. J., Nugent M., Tait C. D., Morris D. E., Heald S. M., Beck K. M., Hess W. P., and Lanzirotti A. (2001) Coprecipitation of uranium(VI) with calcite: XAFS, micro-XAS, nd luminescence characterization. *Geochim. Cosmochim. Acta* **65,** 3491–3503.

Ressler T. (1997) WinXAS: A new software package not only for the analysis of energy-dispersive XAS data. *J. Physique IV* **7,** C2–269.

Rothe J., Denecke M. A., Neck V., Muller R., and Kim J. I. (2002) XAFS investigation of the structure of aqueous thorium(IV) species, colloids, and solid thorium(IV) oxide/hydroxide. *Inorganic Chemistry* **41,** 249–258.

Saini R. D., Bhattacharyya P. K., and Iyer R. M. (1989) Photoluminescence studies of the uranyl carbonate system. *Photochem. Photobiol. A. Chem.* **47,** 65–81.

Savenko A. V. (2001) Sorption of UO_2^{2+} on calcium carbonate. *Radiochemistry* **43,** 193–196.

Thompson H. A., Brown G. E., Jr., and Parks G. A. (1997) XAFS spectroscopic study of uranyl coordination in solids and aqueous solution. *Am. Mineral.* **82,** 483–496.

Waite T. D., Davis J. A., Payne T. E., Waychunas G. A., and Xu N. (1994) Uranium(VI) adsorption to ferrihydrite: Application of a surface complexation model. *Geochim. Cosmochim. Acta* **58,** 5465–5478.